❑   1282

Enhancement of the lighting quality for white light-emitting diodes with CaSc₂O₄:Ce³⁺ phosphor

Phuc Dang Huu[1], Phung Ton That[2], Phan Xuan Le[3], Nguyen Le Thai[4]
[1]Faculty of Fundamental Science, Industrial University of Ho Chi Minh City, Ho Chi Minh City, Vietnam
[2]Faculty of Electronics Technology, Industrial University of Ho Chi Minh City, Ho Chi Minh City, Vietnam
[3]Faculty of Mechanical-Electrical and Computer Engineering, School of Engineering and Technology, Van Lang University,
Ho Chi Minh City, Vietnam
[4]Faculty of Engineering and Technology, Nguyen Tat Thanh University, Ho Chi Minh City, Vietnam

Article Info

ABSTRACT

For the task of realizing greater progress for the light output in white light-emitting diodes (WLEDs), this study focuses on the luminescence temperature subordination feature of $CaSc_2O_4$:Ce^{3+} phosphor (abbreviated to CaS for this study). Some other aspects of the phosphor were also included in this piece of paper: Huang-Rhys coupling factor, stokes shift, triggering power, abatement temperature and especially, abatement behavior in $CaSc_2O_4$:Ce^{3+}. Creating the bluish-green LEDs by the combination of blue InGaN chip and $CaSc_2O_4$:Ce^{3+} is the primary purpose. $CaSc_2O_4$:Ce^{3+} appears to be a decent green phosphor that can be used in WLEDs made of blue InGaN chip. Production tasks may be based on our investigation for the task of making desirable WLED devices that meet the production demands.
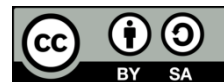
Corresponding Author:

Phan Xuan Le
Faculty of Mechanical-Electrical and Computer Engineering, School of Engineering and Technology
Van Lang University
Ho Chi Minh City, Vietnam
Email: le.px@vlu.edu.vn

1. INTRODUCTION

Due to white light-emitting diodes (WLEDs) characteristics suchlike small power requirement, extended time of use, the lack of mercury, along with ease of repair. They are considered as potential ecologically friendly lighting solutions [1]. The most common WLEDs are the composite containing one LED in blue as well as a yellow phosphor $Y_3Al_5O_{12}$:Ce^{3+} (YAG:Ce^{3+}) [2], [3]. Though, the hue rendering index for such WLED type would be low. We use a mix of green and red phosphors instead of YAG:Ce^{3+} to alleviate this problem [4], [5]. Under blue-light excitation, this type requires high-quantum-efficiency green and red phosphors. Therefore, as a suited and efficient green emitting phosphor, $CaSc_2O_4$:Ce^{3+} was included to serve this purpose. For a LED working under significant energy, the LED generated heat, causing temperature increase of the LED package. Therefore, thermal quenching behavior is a significant attribute. Within that situation, phosphors must be capable of emitting luminosity up to 423 K [6]. Peculiarly, there is a lack of standard studies toward the temperature abatement processes for $CaSc_2O_4$:Ce^{3+} (CaS). Accordingly, our work will investigate in depth the thermal quenching capabilities of CaS. We decided to investigate CaS' abilities when used in WLED devices by combining one 455 nm emitting InGaN chip with CaS to produce a vehement bluish green emitting LED.

2. EXPERIMENTAL

2.1. Preparation of green-emitting $CaSc_2O_4$:Ce^{3+} phosphor

Starting materials consist of $CaCO_3$ (A.R.), CeO_2 (99.99%), as well as Sc_2O_3 (99.99%), with BaF_2 (A.R.) serving as a flux. Based on prior research, we set the ideal Ce^{3+} concentration and BaF_2 content at 0.01 mol and 0.5 wt%[7], resulting in a particle proportion of $CaSc_2O_4$:Ce^{3+} measured at 0.99:2:0.01(Ca:Sc:Ce) during the investigation. In an agate mortar, consolidate all of the initial components and flux. We heated the substance for 1 hour under a temperature of 800 °C in an air atmosphere, then sintered for 6 hours at 1550 °C in an air atmosphere, and finally sintered for more 4 hours at 1450 °C in a reductive atmosphere (25%N_2+75%H_2) [7], [8].

2.2. Charaterization of phosphor

We utilize X-ray powder diffraction (XRD) spectroscopy accompanied by Rigaku D/max 2200 vpc diffractometer and Cu K radiation under 40 kilovolts along with 30 miliamperes to assess the phase purity of the sample. Cas appears to be a singular stage for $CaSc_2O_4$, as seen by the XRD patterns, which are compatible with JCPDS 20-0234. Then, using a Hitachi F7000 spectrofluorometer accompanied by one xenon light working under 450 watts, we measure the temperature dependent photoluminescence emission spectra. A merger was created between the phosphor sample and an InGaN-based blue LED (em=455 nm) for the task of building the LED. Also, we use a PMS-80 LED spectrophotocolorimeter to record the discharge spectra in the LED device operating at various forward-bias direct currents under room temperature (EVERFINE, China). When excited at 460 nm, the Ce^{3+} ions' 5d–4f transition is responsible for the sample's powerful broad peak. As the temperature increases (298-523 K), the emission intensity drops slowly as the full width at half maximum (FWHM) results increase (97-103 nm). With the structural coordinate setting as well as the Boltzmann allocation, the reliance on temperature for FWHM in the discharge of Ce^{3+} may be represented as [9].

$$FWHM(T) = \sqrt{8\ln 2} \times hv \times \sqrt{S} \times \sqrt{coth\left(\frac{hv}{2kT}\right)} \qquad (1)$$

hv represents phonon power. k represents the Boltzmann constant. S represents the Huang-Rhys coupling factor, which assesses the potency for the pairing of electron and phonon. In case S becomes less than one, the coupling is mild; if S is between one and five, the coupling is intermediate; and if S is greater than five, the coupling is strong. As a result, a higher S value suggests a stronger electron-lattice interaction. The $4f^1$ ground status as well as the $4f^05d^1$ excited status in the ions of Ce^{3+} are presumed to have the same hv. Using S value of 1.950, hv value of 0.126 eV, along with R^2 value of 0.99123, the best fit was obtained [10].

The stokes shift can be calculated using the Huang-Rhys parameter and phonon energy. S has a connection with the offset in the parabolas for the structural coordinate graph. It can be determined via (2).

$$\Delta S = (2S - 1) \cdot hv \qquad (2)$$

The stokes shift from (2) for $CaSc_2O_4$:$0.01Ce^{3+}$ phosphor is 0.365 eV (2941 cm^{-1}). Ce^{3+} emission in $CaSc_2O_4$:Ce^{3+} has a smaller stokes shift than discharge of Ce^{3+} within the majority of the remaining structures. Stokes shifts of 1000 to 8000 cm^{-1} seem to be commonly reported. Because of the tiny stokes shift, the Ce^{3+} emission should have a high luminescence quenching temperature. The heat abatement of $CaSc_2O_4$:$0.01Ce^{3+}$ at 460-nm optical stimulation was examined with a temperature limit of 298 K - 523 K. Under around 423 K, the intensity of discharge in Ce^{3+} rapidly decrease. The temperature of heat abatement, with intensity of discharge being half of that under room temperature, would be around 530 K. For high-power white LEDs, the $CaSc_2O_4$:Ce^{3+} phosphor is ideal. To quench f-d emission of Ce^{3+}, we can utilize the heat-triggered cross-over ($4f^05d^1$ excited status to $4f^1$ ground status, or heat-triggered photoionization ($4f^05d^1$ status to conducting line) [11]. When the stokes shift of the f-d discharge, as well as the phosphor's temperature of abatement, becomes small, photoionization becomes the reason for the phosphor's temperature quenching. Both mechanisms are indispensable in the heat abatement for CaS because the stokes shift appears to be minor. On the other hand, the temperature of luminescence abatement appears to be comparatively significant. Taking heat abatement theory into account, it is possible to determine the intensity that correlates with temperature via an equation [12]-[14].

$$I(T) = \frac{I(0)}{1 + A exp(-\Delta E/kT)} \qquad (3)$$

In the equation, $I(0)$ represents the first intensity under room temperature, and $I(T)$ represents the intensity under one specific temperature. T represents the time constant. A represents the triggering power. E represents the activation energy. k is the Boltzmann constant. With $R^2 = 0.99855$, A and E were calculated to be around 473.992 and 0.282 eV, respectively, using the aforementioned equation.

We created a pc-LED (LED device based on conversion phosphor) through mixing a chip of LED

under 455 nm accompanied by CaS to examine the possible application for CaS in white LEDs. The electroluminescence spectrum in a green-light diode based on conversion phosphor at forwarding bias direct currents measured at 10, 20, 30, 40, 50, 100, 150, 200, 250, 300, as well as 350 milliamperes. Excitation with blue light from an LED chip produces one wide discharge line accompanied by one peak reaching 517 nm. Meanwhile, the discharge under 455 nm within the device is still visible. Under surging forward-bias direct current between 10 and 350 milliamperes, the electroluminescent intensity under discharges measured at 455 nm as well as 517 nm increases concurrently without being saturated. The outcome shows that CaS possesses exceptional luminous characteristics. The sheet of phosphor in the MCW-LEDs can be replicated using level silicone layers using the LightTools 9.0 application and the Monte Carlo approach [15]-[17]. This simulation takes place through separate stages. The first stage is about establishing as well as create MCW-LED lamp configuration models and optical characteristics. The second stage involves controlling the optical influences from phosphor compounding via the $CaSc_2O_4:Ce^{3+}$ content variety. We must establish several contrasts in order to determine the influence from $YAG:Ce^{3+}$ as well as CaS imposed on the output in the MCW-LED device. Dual-layer distant phosphorus, described as two types of compounds with average CCTs of 3000 K, 4000 K, and 5000 K, is to be elucidated. Figure 1 depicts MCW-LED lamps containing conformal mixture of phosphor under 8500-K CCT in detail. The simulation of MCW-LEDs without CaS is also recommended. The reflector's bottom length, height, as well as length of the top surface, are shown as follows: 8 mm, 2.07 mm, 9.85 mm. The mentioned mixture is applied to nine chips that are 0.08 mm thick. All of them are connected to the reflector cavity by a square base measured at 1.14 mm2 along with a height measured at 0.15 mm. All chips in blue possess a radiant flux measured at 1.16 watts, with an apex wavelength of 453 nm.
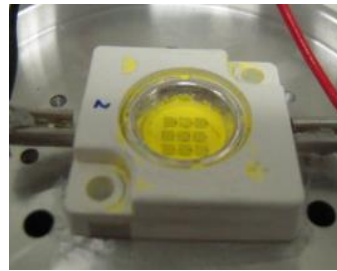

Figure 1. Photograph of WLEDs

3. RESULTS AND ANALYSIS

Figure 2 exhibits the reversal shift in the concentrations of $CaSc_2O_4:Ce^{3+}$ along with $YAG:Ce^{3+}$. Such adjustment has the following purposes: keeping median CCT values, and affecting the absorptivity as well as the dispersion in the WLED device with a pair of phosphor sheets. This, in turn, has effects on both color performance and lumen intensity of the device. The device's hue quality is thus determined by the $CaSc_2O_4:Ce^{3+}$ concentration chosen. When the $CaSc_2O_4:Ce^{3+}$ ratio increased (5% - 15% Wt.), the $YAG:Ce^{3+}$ content decreased for the purpose of sustaining median CCT values. Moreover, through comparing the concentration data of the WLEDs having 5000 K and 5700 K as shown in Figure 2(a) and 2(b) with that of the 6500 K and 8000 K WLEDs as shown in Figure 2(c) and 2(d), the packages with color temperatures CCTs >6000 K result in much lower $YAG:Ce^{3+}$ concentration as $CaSc_2O_4:Ce^{3+}$ increases, meaning that impacts of $CaSc_2O_4:Ce^{3+}$ on the lighting efficiency of high-CCT WLEDs could be more significant.

Figure 3 shows the influence of the $CaSc_2O_4:Ce^{3+}$ green phosphorus concentration on the transmitting spectrum in the WLED device. We can pick the best option by considering the producer's requirements. The WLED devices that demand good chromatic fidelity may diminish luminous flux slightly. As seen in Figure 3, white illumination is synthesized via the area of spectrum. The spectra for these four numbers would be 5000 K, 5700 K, 6500 K, and 8000 K, respectively. The intensity will be proportional to the $CaSc_2O_4:Ce^{3+}$ concentration of two sections in the light spectrum: 420-480 nm along with 500-640 nm. Such a rise of the final value for luminous flux is illustrated in the discharge spectrum with two lines. The surge of blue-light scattering in WLEDs implies some followers in the color uniformity, phosphorous layer, and WLEDs' scattering. This is considered a notable outcome of the $CaSc_2O_4:Ce^{3+}$ application. The color consistency for the distant phosphor layout under significant temperatures will be challenging to control. Our assessment found that $CaSc_2O_4:Ce^{3+}$, under color temperatures of 5600 K as well as 8500 K, can provide greater hue output for WLED devices.
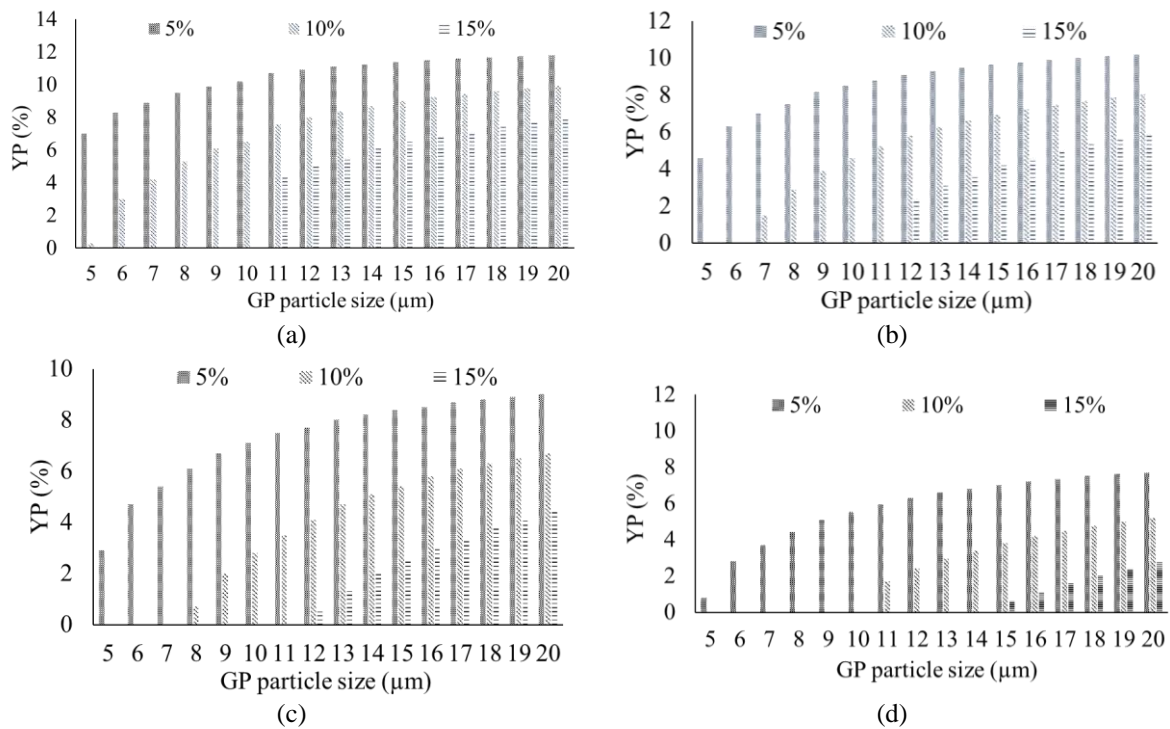
Figure 2. Alter phosphor content for the task of retaining median CCTs of (a) 5000 K, (b) 5700 K,
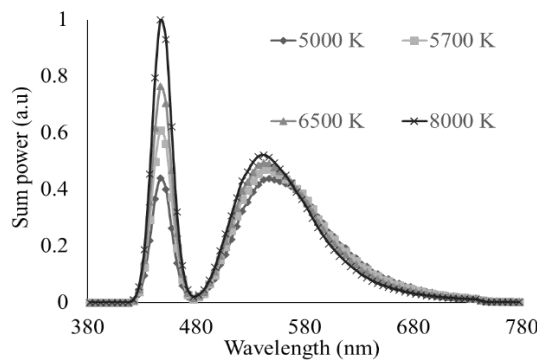(c) 6500 K, and (d) 8000 K

Figure 3. The emission spectra in the WLED device as a function of $CaSc_2O_4:Ce^{3+}$ concentration

The performance in the emitted light flux from the emote phosphor layout with a pair of phosphor sheets was further exhibited. The results in Figure 4 show that as CaS content increases (5% wt. - 15% wt.), the lumen increases notably. Moreover, according to Figures 4(a), 4(b), 4(c), as well as 4(d), the luminous fluxes would be relatively the same between the four CCTs, showing that the CaS green phosphor enables the luminous stability of the WLED when switching from lower (5000-5700 K) to higher (6500 – 8000 K) CCTs. Additionally, in all four average CCTs, the color differences considerably declined with the phosphor $CaSc_2O_4:Ce^{3+}$ presence, as shown in Figure 5. Such an outcome is possibly the result of the $CaSc_2O_4:Ce^{3+}$ phosphor sheet's absorption. When the blue light generated by the chip in LED gets absorbed via CaS, it will turn into green illumination. The yellow illumination is absorbed by the $CaSc_2O_4:Ce^{3+}$ particles, besides the blue light mentioned, but this yellow-light absorption is not as strong as the blue one, owing to the absorption characteristics of the phosphor [18]-[20]. By adding CaS, the presence of green illumination surges in the WLED device, improving the color uniformity index. Hue consistency would be an extremely crucial facet among current WLED parameters. The higher the ue consistency, the greater the price of WLED. However, the low cost of CaS would be an advantage $CaSc_2O_4:Ce^{3+}$ can thus be used in a variety of applications.
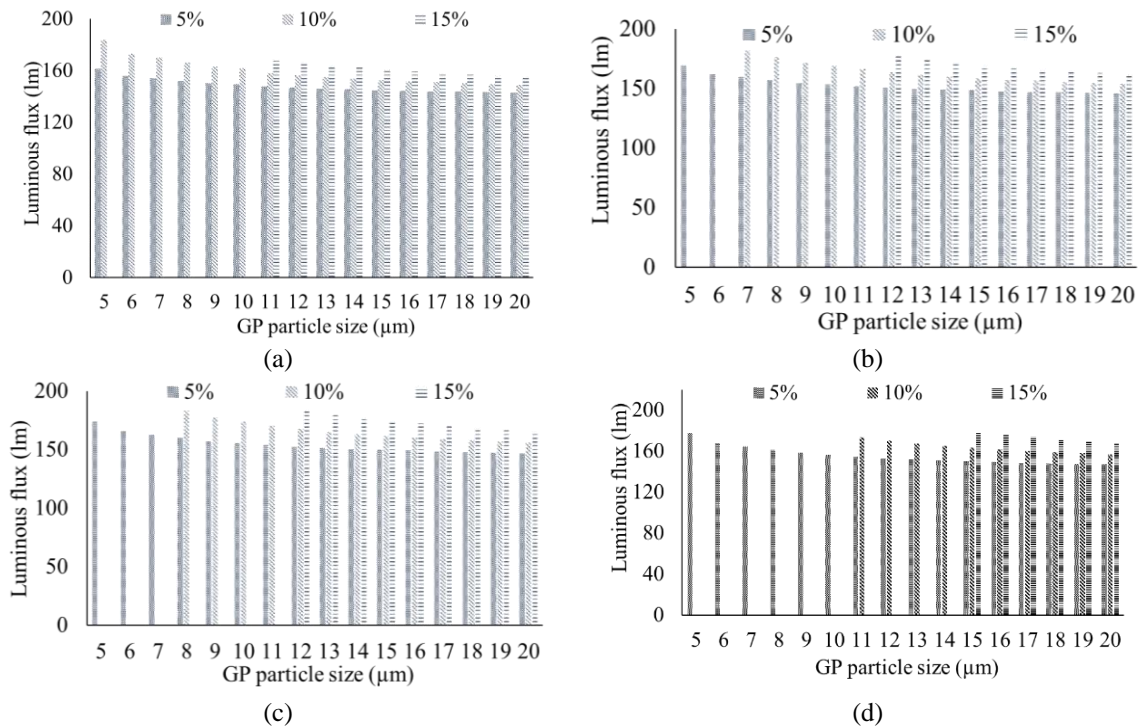
Figure 4. The lumen in the WLED device accompanied by CaS content at (a) 5000 K, (b) 5700 K,
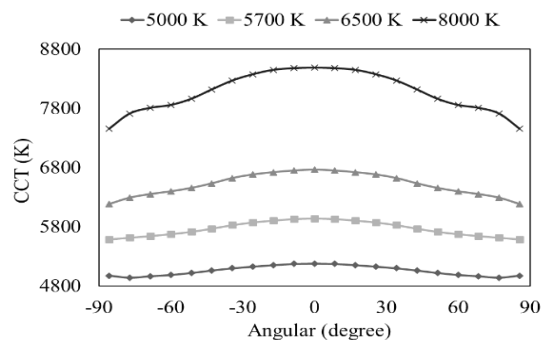(c) 6500 K, and (d) 8000 K

Figure 5. CCT in the WLED device accompanied by CaS content

It needs more than good color uniformity to give a more thorough chromatic evaluation for a WLED. In other words, it is not possible to guarantee good color quality using significant hue consistency alone. As a result, newer investigations have developed a color rendering index (CRI) as well as a color quality scale (CQS) [21]-[23]. If light shines on the CRI, it determines an entity's authentic hue. When the green illumination between the principal colors (blue, yellow, and green) becomes too abundant, it causes color imbalance, making the fidelity in color output decrease. The outcomes shown in Figure 6 show one small CRI penalty in the presence of the distant phosphor $CaSc_2O_4:Ce^{3+}$ layer. When the concentration of CaS increases 15% wt., the CRI particularly reduces to around 50 in all four CCTs of 5000 K, 5700 K, 6500 K, and 8000 K, as in Figures 6(a), 6(b), 6(c), as well as 6(d), respectively. Nonetheless, these downsides are somehow allowed because comparing CRI with CQS, the latter needs to be focused on. It takes into account certain indexes: CRI, observer's preference, along with chromatic coordinate [24], [25]. Hence, this parameter becomes a genuine overall assessment of chromatic quality.

Figure 7 shows the parameter's increase with the remote $CaSc_2O_4:Ce^{3+}$ sheet's presence. Furthermore, when the concentration of $CaSc_2O_4:Ce^{3+}$ gets raised, CQS does not change considerably when CaS content is under 10% wt. and larger particle sizes are applied. Besides, the CQS changes are insignificant when the CCT of the WLED is at 5000 K, see Figure 7(a). When the CCT increases the

differences in CQS per CaS concentration become more noticeable, especially in the cases of using small CaS particle sizes, as demonstrated by Figures 7(b), 7(c), as well as 7(d). CRI and CQS become diminished noticeably when CaS concentrations are larger than 10% wt. This is the result of severe waste of hue if green becomes dominant. Utilizing CaS will require determining the right concentration.
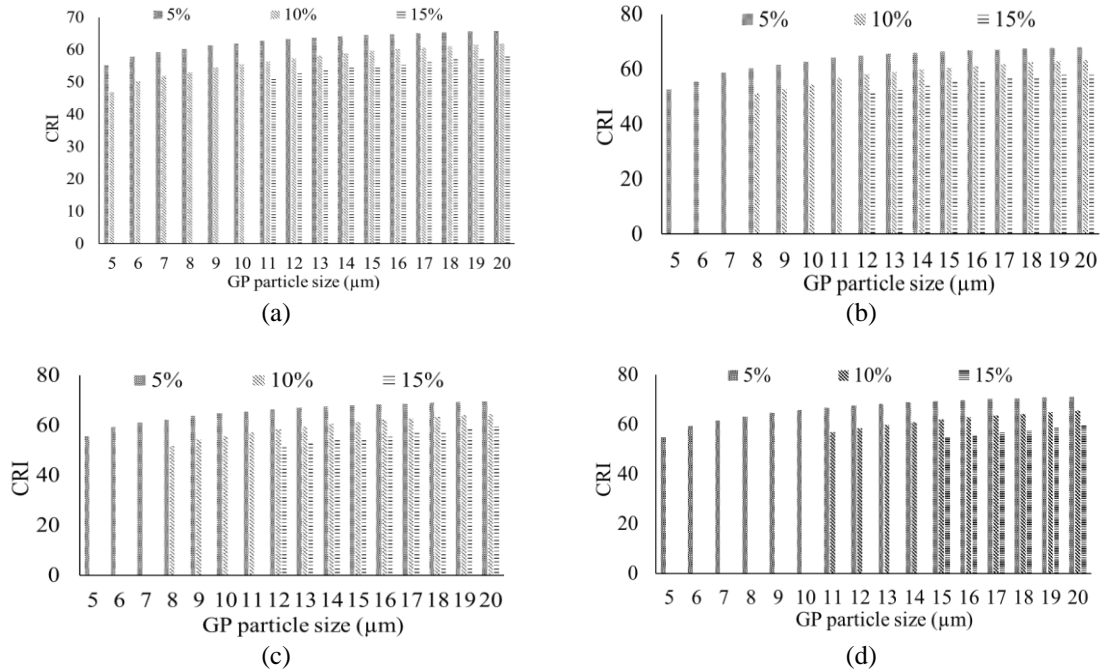

Figure 6. CRI in the WLED device accompanied by CaS content at (a) 5000 K, (b) 5700 K, (c) 6500 K, and (d) 8000 K
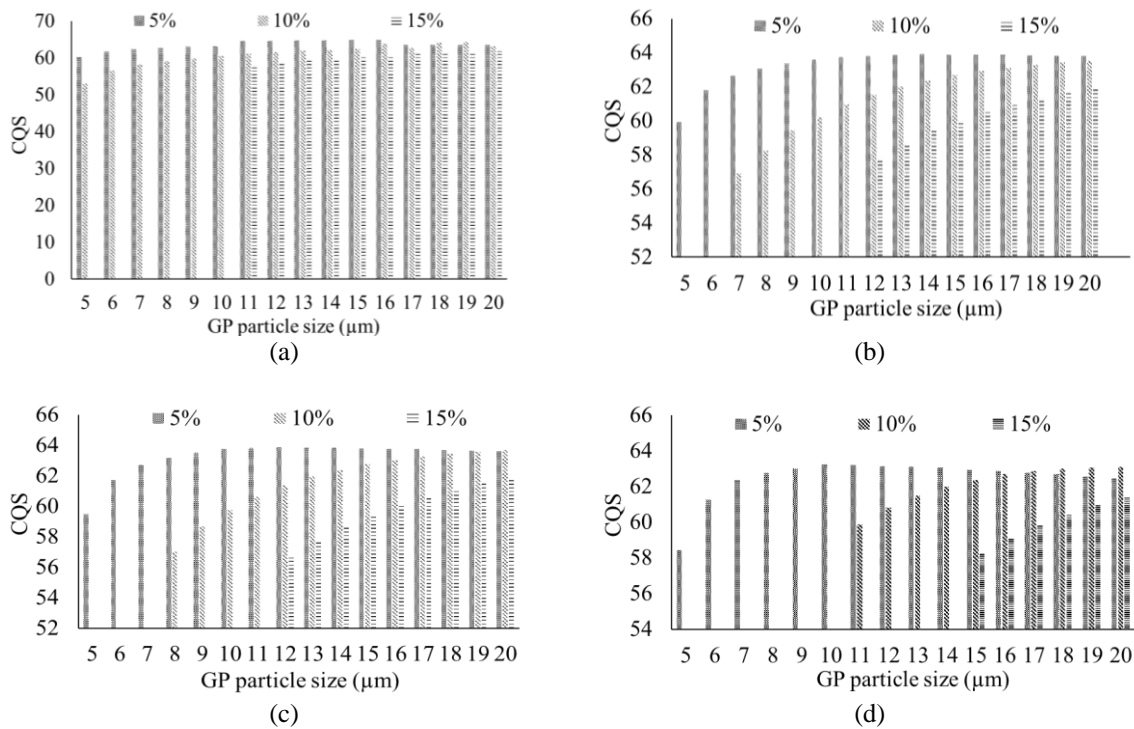
Figure 7. CQS in the WLED device accompanied by CaS content at (a) 5000 K, (b) 5700 K, (c) 6500 K, and (d) 8000 K

4. CONCLUSIONS

The solid-state reaction approach was used to make the green-emitting CaS phosphor. From 298 to 523 K, the temperature-dependent luminous characteristics of CaS phosphor were examined. The CaS' discharge line exhibits an inferior intensity of discharge as well as a greater apex FWHM as temperature rises. 1.950, 0.365 eV, 0.282 eV, as well as 530 K were found to represent the Huang-Rhys coupling factor, stokes shift, triggering power, as well as temperature of abatement in CaS phosphors, respectively. As the forward-bias current fluctuates up to 350 mA, the manufactured LED exhibits outstanding chromaticity without saturation. CaS might become a decent choice for green phosphor in WLED devices.

ACKNOWLEDGEMENTS

REFERENCES

[1] R. Dolenec, L. Rogelj, J. Stergar, and M. Milanic, "Modular multi-wavelength LED based light source for hyperspectral imaging," *Clinical and Preclinical Optical Diagnostics II*, vol. EB101, pp. 11075-56, 2019, doi: 10.1117/12.2527075.

[2] S. K. Abeysekera, S. Khyle, V. Kalavally, M. Ooi, and Y. C. Kuang, "Impact of circadian tuning on the illuminance and color uniformity of a multichannel luminaire with spatially optimized LED placement," *Vineetha Kalavally,* vol. 28, pp.130-145, 2020, doi: 10.1364/OE.381115.

[3] K. W. Houser, "The problem with luminous efficacy," *LEUKOS*, vol. 16, pp. 97, 2020, doi: 10.1080/15502724.2019.1704605.

[4] Q. Yao, L. Zhang, Q. Dai, and J. Uttley, "Quantification of trichromatic light sources to achieve tunable photopic and mesopic luminous efficacy of radiation," *LEUKOS*, vol. 15, pp. 271-280, 2019, doi: 10.1080/15502724.2018.1531719.

[5] M. U. F. Shahnia, G. M. Shafiullah, and A. Arefi, "Utility and consumer-oriented multi-criteria assessment of residential light bulbs available on the Australian market," *Australian Journal of Electrical and Electronics Engineering*, vol. 15, pp. 38-52, 2018, doi: 10.1080/1448837X.2018.1499173.

[6] D. Durmus, D. Abdalla, A. Duis, and W. Davis, "Spectral optimization to minimize light absorbed by artwork," *LEUKOS,* vol. 16, pp. 45-54, 2020, doi: 10.1080/15502724.2018.1533852.

[7] N. A. Vaz and M. Inanici, "Syncing with the sky: daylight-driven circadian lighting design," *LEUKOS*, vol. 17, pp. 291-309, 2021, doi: 10.1080/15502724.2020.1785310.

[8] H. W. Wang, I. Neretnieks, and M. Voutilainen, "A note on the use of uranine tracer to visualize radionuclide migration experiments: some observations and problems," *Nuclear Technology*, vol. 205, pp. 964-977, 2019, doi: 10.1080/00295450.2019.1573620.

[9] J. H. Han, I. Neretnieks, and M. Voutilainen, "Luminescence enhancement of OLED lighting panels using a microlens array film," *Journal of Information Display*, vol. 19, pp. 179-184, 2018, doi: 10.1080/15980316.2018.1531073.

[10] K. W. Houser, "Lighting standards: when is doing something, better than doing nothing?," *LEUKOS*, vol. 16, pp. 251-253, 2020, doi: 10.1080/15502724.2020.1741963.

[11] Z. Zhao, H. Zhang, S. Liu, and X. Wang, "Effective freeform TIR lens designed for LEDs with high angular color uniformity," *Applied Optics*, vol. 57, no. 15, pp. 4216-4221, 2018, doi: 10.1364/AO.57.004216.

[12] H. Yu *et al.,* "Solar spectrum matching with white OLED and monochromatic LEDs," *Applied Optics*, vol. 57, no. 10, pp. 2659-2666, 2018, doi: 10.1364/AO.57.002659.

[13] N. Anous, T. Ramadan, M. Abdallah, K. Qaraqe, and D. Khalil, "Impact of blue filtering on effective modulation bandwidth and wide-angle operation in white LED-based VLC systems," *OSA Continuum*, vol. 1, no. 3, pp. 910-929, 2018, doi: 10.1364/OSAC.1.000910.

[14] H. Ke *et al.,* "Lumen degradation analysis of LED lamps based on the subsystem isolation method," *Applied Optics*, vol. 57, no. 4, pp. 849-854, 2018, doi: 10.1364/AO.57.000849.

[15] H. Lee *et al.,* "Color-tunable organic light-emitting diodes with vertically stacked blue, green, and red colors for lighting and display applications," *Optics Express*, vol. 26, no. 14, pp. 18351-18361, 2018, doi: 10.1364/OE.26.018351.

[16] J. O. Kim, H. S. Jo, and U. C. Ryu, "Improving CRI and scotopic-to-photopic ratio simultaneously by spectral combinations of CCT-tunable LED lighting composed of multi-chip LEDs," *Current Optics and Photonics*, vol. 4, no. 3, pp. 247-252, 2020, doi: 10.1364/COPP.4.000247.

[17] H. S. El-Ghoroury, Y. Nakajima, M. Yeh, E. Liang, C. L. Chuang, and J. C. Chen, "Color temperature tunable white light based on monolithic color-tunable light emitting diodes," *Optics Express*, vol. 28, no. 2, pp. 1206-1215, 2020, doi: 10.1364/OE.375320.

[18] Y. W. Y. Zhang, D. Li, A. Zhang, H. Wang, H. Jia, and B. Xu, "Tunable white light emission of an anti-ultraviolet rare-earth polysiloxane phosphors based on near UV chips," *Optics Express*, vol. 29, no. 6, pp. 8997-9011, 2021, doi: 10.1364/OE.410154.

[19] M. Gupta, A. K. Dubey, V. Kumar, and D. S. Mehta, "Indoor daylighting using fresnel lens solar-concentrator-based hybrid cylindrical luminaire for illumination and water heating," *Applied Optics*, vol. 59, no. 18, pp. 5358-5367, 2020, doi: 10.1364/AO.389044.

[20] A. Ali *et al.,* "Blue-laser-diode–based high CRI lighting and high-speed visible light communication using narrowband green-red-emitting composite phosphor film," *Applied Optics*, vol. 59, no. 17, pp. 5197-5204, 2020, doi: 10.1364/AO.392340.

[21] X. Liu *et al.,* "Laser-based white-light source for high-speed underwater wireless optical communication and high-efficiency underwater solid-state lighting," *Optics Express*, vol. 26, no. 15, pp. 19259-19274, 2018, doi: 10.1364/OE.26.019259.

[22] R. Fan, S. Fang, C. Liang, Z. Liang, and H. Zhong, "Controllable one-step doping synthesis for the white-light emission of cesium copper iodide perovskites," *Photonics Research*, vol. 9, no. 5, pp. 694-700, 2021, doi: 10.1364/PRJ.415015.

[23] S. Donati, W. H. Cheng, C. N. Liu, H. K. Shih, and Z. Pei, "Embedding LiDAR and smart laser headlight in a compact module for autonomous driving," *OSA Continuum*, vol. 4, no. 5, pp. 1587-1597, 2021, doi: 10.1364/OSAC.424159.

[24] Y. P. Chang, J.-K. Chang, H.-A. Chen, S.-H. Chang, C.-N. Liu, P. Han, and W.-H. Cheng, "An advanced headlight module employing highly reliable glass phosphor," *Optics Express*, vol. 27, no. 3, pp. 1808-1815, 2019, doi: 10.1364/OE.27.001808.

[25] Y. Sun, C. Zhang, Y. Yang, H. Ma, and Y. Sun, "Improving the color gamut of a liquid-crystal display by using a bandpass filter," *Current Optics and Photonics*, vol. 3, no. 6, pp. 590-596, 2019, doi: 10.1364/COPP.3.000590.

BIOGRAPHIES OF AUTHORS

Phuc Dang Huu received a Physics Ph.D degree from the University of Science, Ho Chi Minh City, in 2018. Currently, he is a lecturer at the Faculty of Fundamental Science, Industrial University of Ho Chi Minh City, Ho Chi Minh City, Vietnam. His research interests include simulation LEDs material, renewable energy. He can be contacted at email: danghuuphuc@iuh.edu.vn.

Phung Ton That was born in Thua Thien-Hue, Vietnam. He received the B.Sc. degree in electronics and telecommunications engineering (2007) and the M.Sc. degree in electronics engineering (2010) from the University of Technology, Vietnam. He is currently a lecturer at the Faculty of Electronics Technology (FET), Industrial University of Ho Chi Minh City. His research interests are optical materials, wireless communication in 5G, energy harvesting, performance of cognitive radio, physical layer security and NOMA. He can be contacted at email: tonthatphung@iuh.edu.vn.

Phan Xuan Le received a Ph.D. in Mechanical and Electrical Engineering from Kunming University of Science and Technology, Kunming city, Yunnan province, China. Currently, He is a lecturer at the Faculty of Engineering, Van Lang University, Ho Chi Minh City, Viet Nam. His research interests are Optoelectronics (LED), Power transmission and Automation equipment. He can be contacted at email: le.px@vlu.edu.vn.

Nguyen Le Thai received his BS in Electronic engineering from Danang University of Science and Technology, Vietnam, in 2003, MS in Electronic Engineering from Posts and Telecommunications Institute of Technology, Ho Chi Minh, Vietnam, in 2011 and PhD degree of Mechatronics Engineering from Kunming University of Science and Technology, China, in 2016. He is a currently with the Nguyen Tat Thanh University, Ho Chi Minh City, Vietnam. His research interests include the renewable energy, optimisation techniques, robust adaptive control and signal processing. He can be contacted at email: nlthai@nttu.edu.vn.